Supporting Information:

"Convolutional Neural Network of Atomic Surface Structures to Predict Binding Energies for High-throughput Screening of Catalysts"

Seoin Back,[†,‡] Junwoong Yoon,[†,‡] Nianhan Tian,[†] Wen Zhong,[†] Kevin Tran,[†] and Zachary W. Ulissi[*,†]

†*Department of Chemical Engineering, Carnegie Mellon University, Pittsburgh, PA, USA*

‡*These authors contributed equally to this work.*

E-mail: zulissi@andrew.cmu.edu

Table S1. Hyperparameters of convolutional neural network optimized by Sigopt.

Parameters	CO binding energies	H binding energies
Batch size	214	140
Learning rate	5.6×10^{-3}	9.9×10^{-4}
Epochs	150	150
atom_fea_len	46	107
h_fea_len	83	50
n_conv	8	6
n_h	4	1

Table S2. The components of parameters in the convolutional network.

CO							
embedding.weight	46	convs.2.bn1.bias	92	convs.5.bn1.weight	92	conv_to_fc.bias	83
embedding.bias	46	convs.2.bn2.weight	46	convs.5.bn1.bias	92	fcs.0.weight	83
convs.0.fc_full.weight	92	convs.2.bn2.bias	46	convs.5.bn2.weight	46	fcs.0.bias	83
convs.0.fc_full.bias	92	convs.3.fc_full.weight	92	convs.5.bn2.bias	46	fcs.1.weight	83
convs.0.bn1.weight	92	convs.3.fc_full.bias	92	convs.6.fc_full.weight	92	fcs.1.bias	83
convs.0.bn1.bias	92	convs.3.bn1.weight	92	convs.6.fc_full.bias	92	fcs.2.weight	83
convs.0.bn2.weight	46	convs.3.bn1.bias	92	convs.6.bn1.weight	92	fcs.2.bias	83
convs.0.bn2.bias	46	convs.3.bn2.weight	46	convs.6.bn1.bias	92	bn.0.weight	83
convs.1.fc_full.weight	92	convs.3.bn2.bias	46	convs.6.bn2.weight	46	bn.0.bias	83
convs.1.fc_full.bias	92	convs.4.fc_full.weight	92	convs.6.bn2.bias	46	bn.1.weight	83
convs.1.bn1.weight	92	convs.4.fc_full.bias	92	convs.7.fc_full.weight	92	bn.1.bias	83
convs.1.bn1.bias	92	convs.4.bn1.weight	92	convs.7.fc_full.bias	92	bn.2.weight	83
convs.1.bn2.weight	46	convs.4.bn1.bias	92	convs.7.bn1.weight	92	bn.2.bias	83
convs.1.bn2.bias	46	convs.4.bn2.weight	46	convs.7.bn1.bias	92	visualization_layer.weight	1
convs.2.fc_full.weight	92	convs.4.bn2.bias	46	convs.7.bn2.weight	46	visualization_layer.bias	1
convs.2.fc_full.bias	92	convs.5.fc_full.weight	92	convs.7.bn2.bias	46	fc_out.weight	1
convs.2.bn1.weight	92	convs.5.fc_full.bias	92	conv_to_fc.weight	83	fc_out.bias	1

| H							
embedding.weight	107	convs.1.bn1.bias	214	convs.3.bn1.weight	214	convs.5.fc_full.bias	214
embedding.bias	107	convs.1.bn2.weight	107	convs.3.bn1.bias	214	convs.5.bn1.weight	214
convs.0.fc_full.weight	214	convs.1.bn2.bias	107	convs.3.bn2.weight	107	convs.5.bn1.bias	214
convs.0.fc_full.bias	214	convs.2.fc_full.weight	214	convs.3.bn2.bias	107	convs.5.bn2.weight	107
convs.0.bn1.weight	214	convs.2.fc_full.bias	214	convs.4.fc_full.weight	214	convs.5.bn2.bias	107
convs.0.bn1.bias	214	convs.2.bn1.weight	214	convs.4.fc_full.bias	214	conv_to_fc.weight	50
convs.0.bn2.weight	107	convs.2.bn1.bias	214	convs.4.bn1.weight	214	conv_to_fc.bias	50
convs.0.bn2.bias	107	convs.2.bn2.weight	107	convs.4.bn1.bias	214	visualization_layer.weight	1
convs.1.fc_full.weight	214	convs.2.bn2.bias	107	convs.4.bn2.weight	107	visualization_layer.bias	1
convs.1.fc_full.bias	214	convs.3.fc_full.weight	214	convs.4.bn2.bias	107	fc_out.weight	1
convs.1.bn1.weight	214	convs.3.fc_full.bias	214	convs.5.fc_full.weight	214	fc_out.bias	1
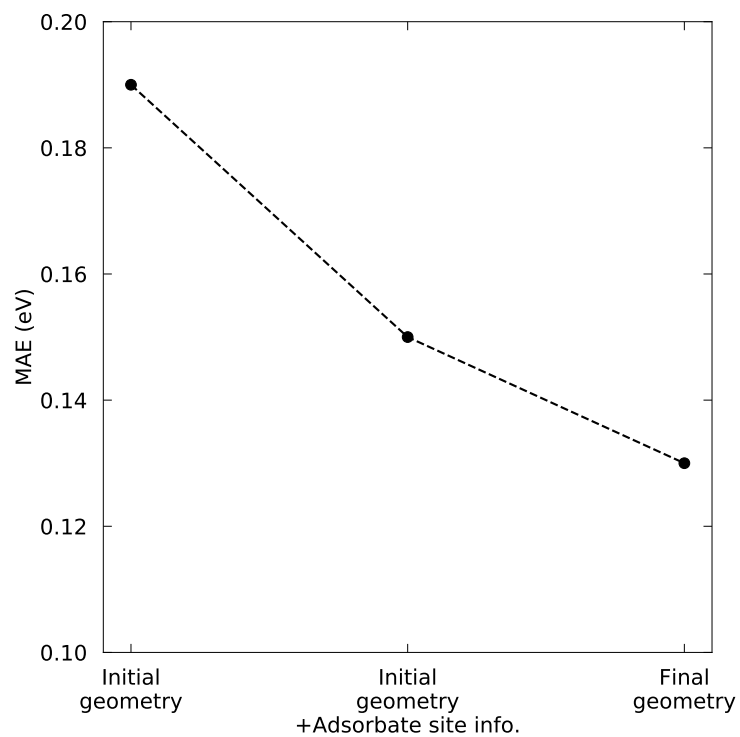
Figure S1: Prediction performance of training with initial structures only, final structures only, and initial structures with the connectivity distance information of adsorbates obtained from the final structures. MAE values of test sets are presented. For the rest of this work, we used the results trained with initial structures with adsorbate distance information.
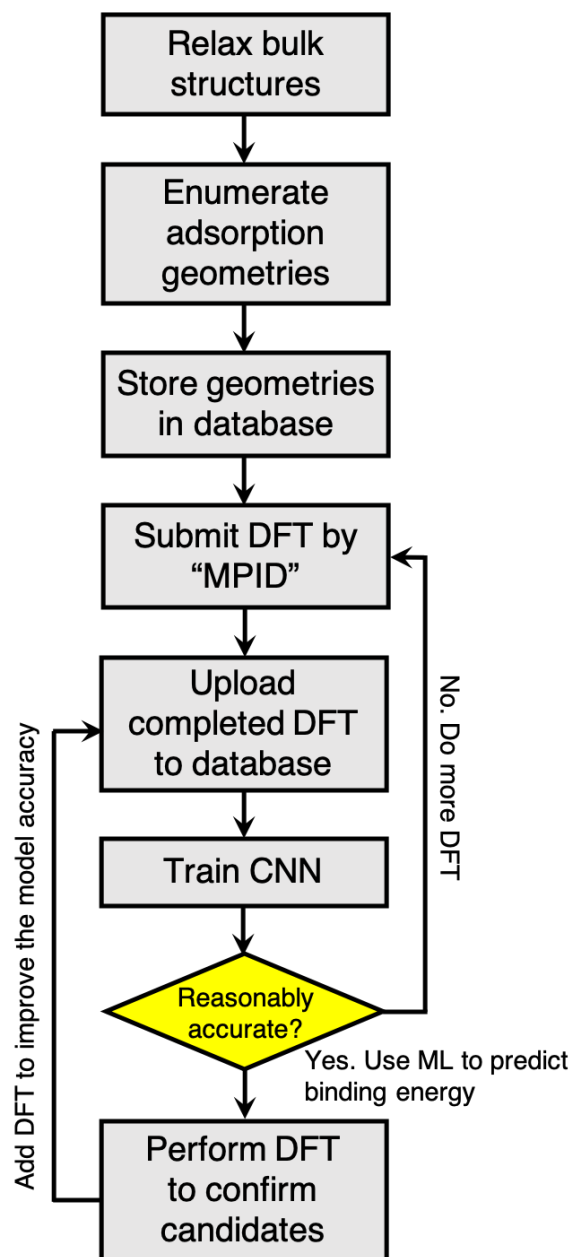
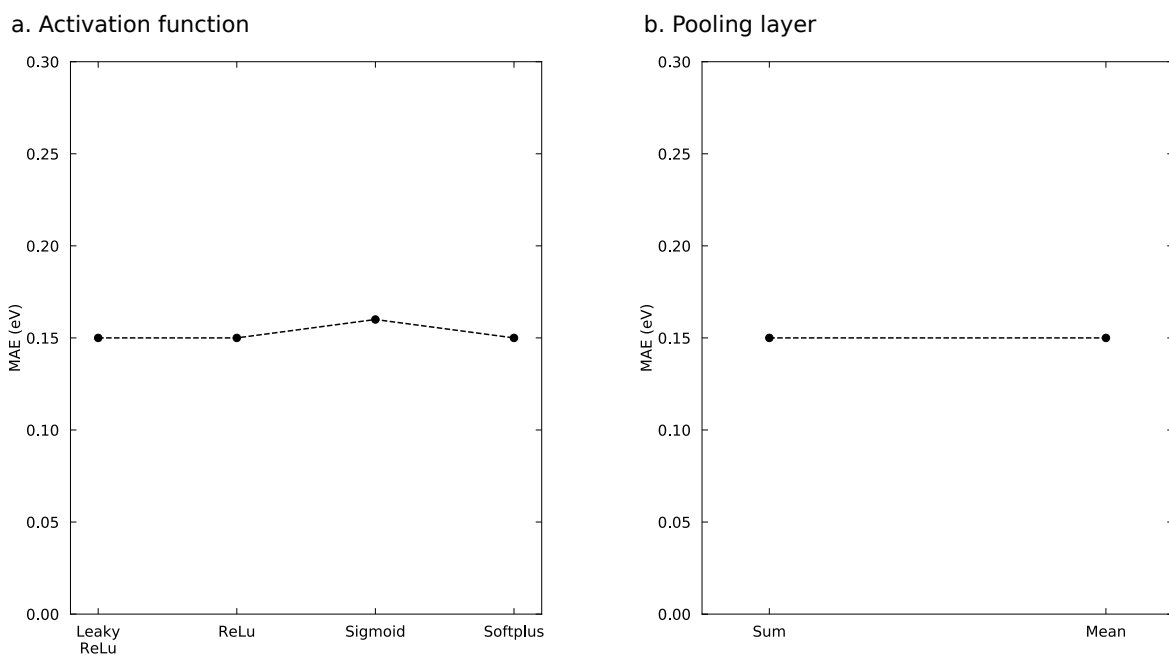Figure S2: A process of high-throughput workflow for the catalyst screening.

a. Activation function

b. Pooling layer

Figure S3: Prediction performance depending on (a) activation functions and (b) pooling layers. MAE values of test sets are presented.

Atom Feature

Embedding (46)

fc_full (92)

bn1 (92)

bn2 (46)

X 8

conv_to_fc (83)

fcs (83)

bn (83)

X 3

visualization_layer (1)

Pooling
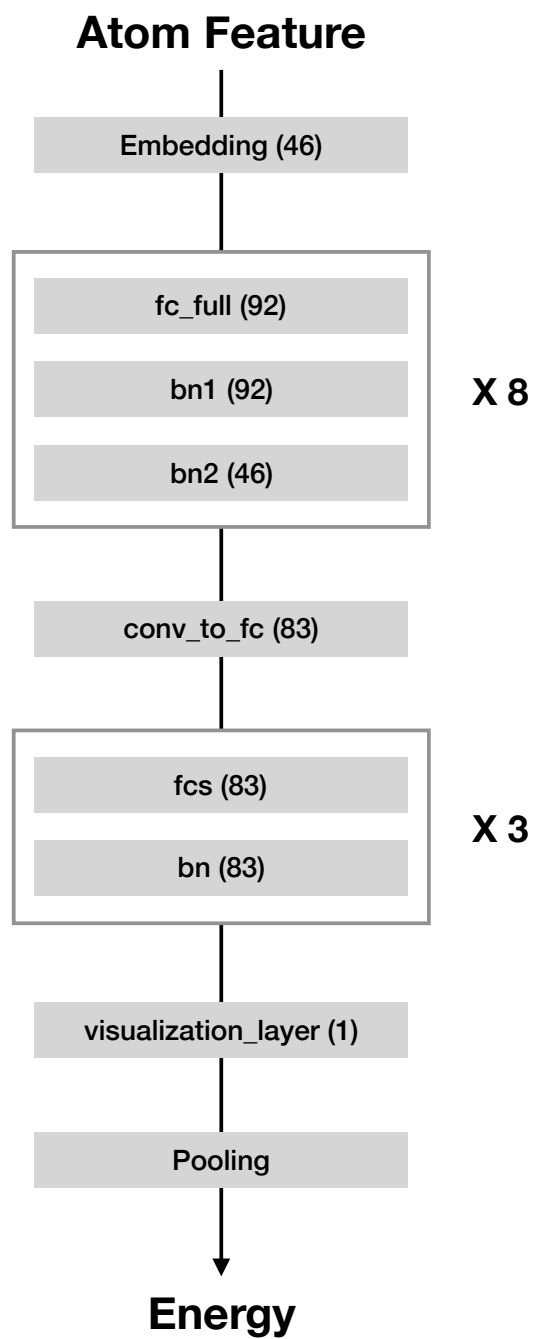
Energy

Figure S4: Convolutional neural network architecture used in this work. The values in parenthesis correspond to the number of parameters for CO binding energy prediction (Table S2).
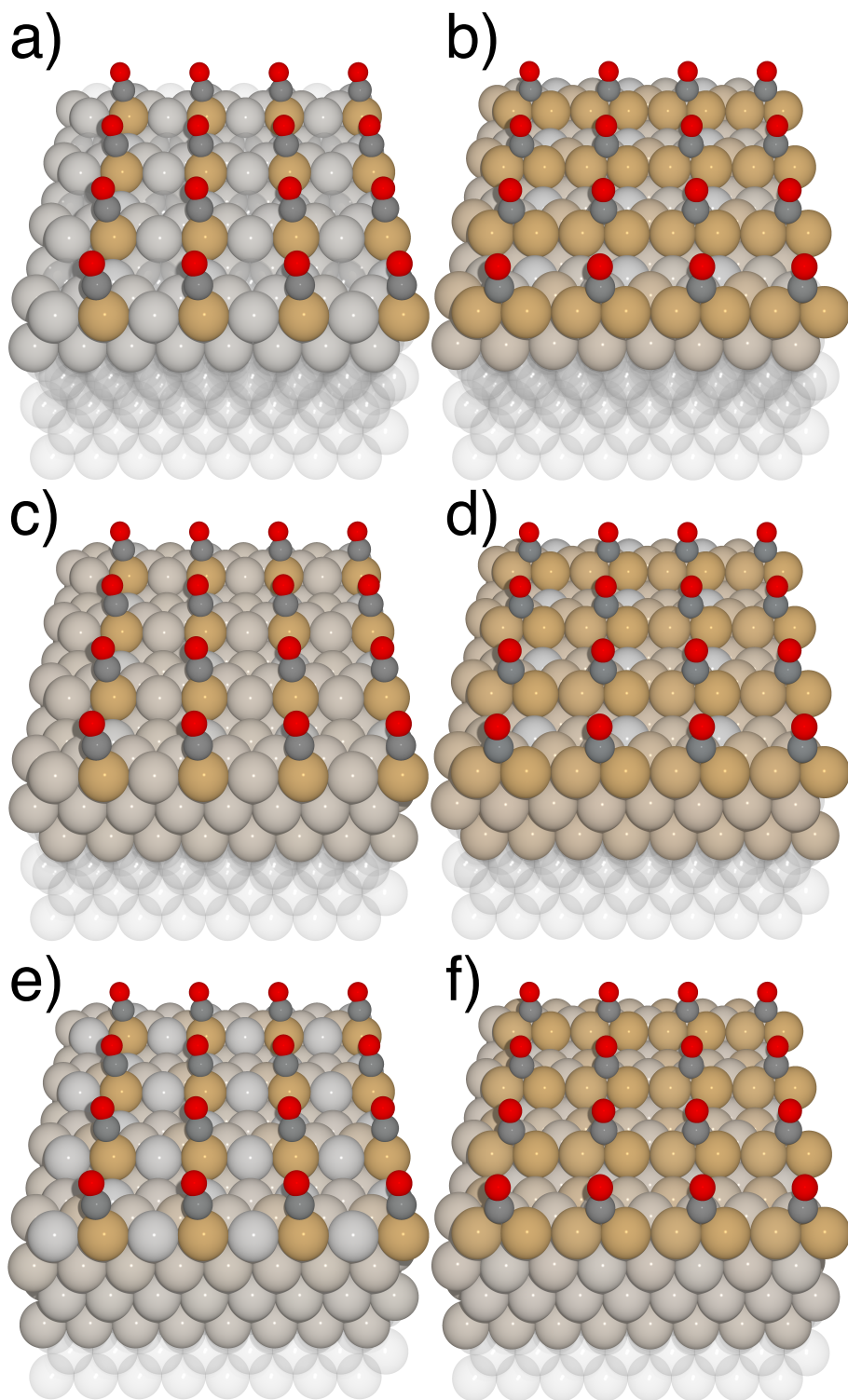
Figure S5: Comparison of different connectivity distance cutoff values: (a,b) 2, (c,d) 3, (e,f) 4 for CO adsorption on Cu (211) surface. (a,c,e) and (b,d,f) correspond to CO binding on top and bridge site, respectively. Atoms with the distance 3 and 4 contribute negligibly to the binding energies. Transparent balls indicate atoms with connectivity distances higher than the cutoffs.
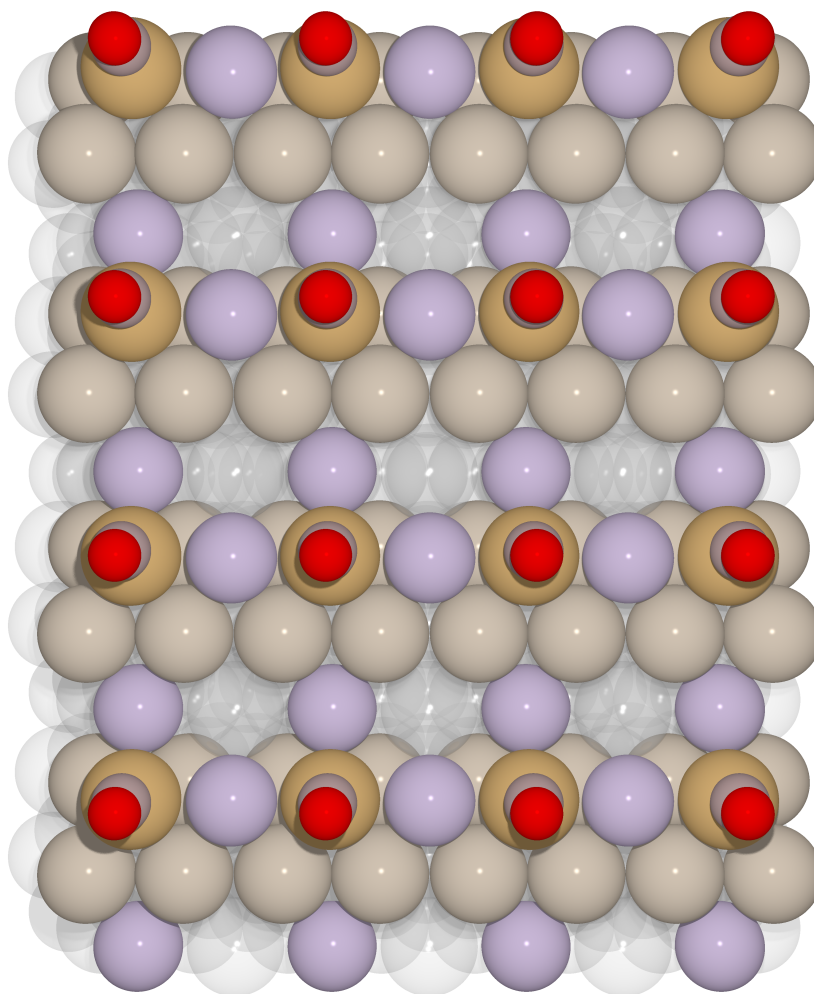
Figure S6: Top view of CO adsorption on Cu$_3$Al (211) surface. Darker spheres indicate higher contributions. Dark brown spheres are Cu atoms directly interacting with CO adsorbate (distance = 1), light grey spheres are Cu atoms not interacting with the CO (distance = 2). Lilac spheres are Al (distance = 2). Transparent spheres indicate atoms with connectivity distances higher than 2.
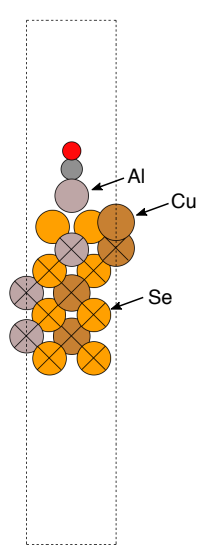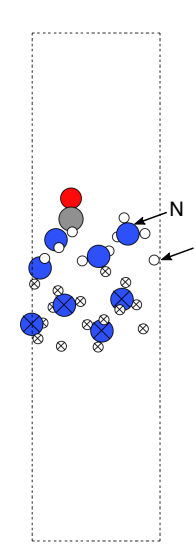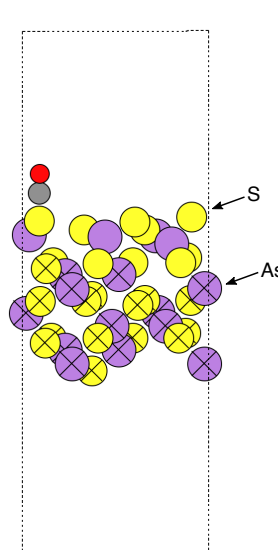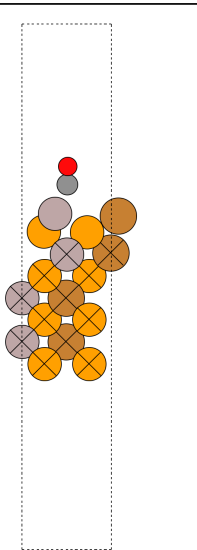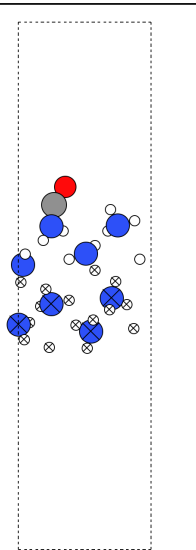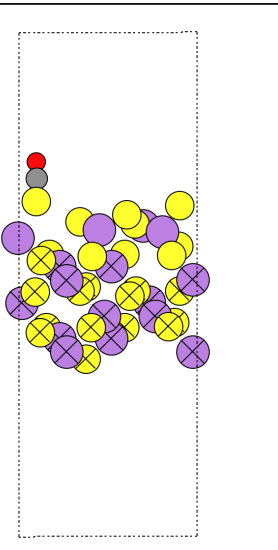
1) Surface reconstruction	2) Wrong initial structure	3) Desorption of surface atom
mp-8016, [0,0,1] 0.06, True	mp-29145, [1,1,0] 0.09, True	mp-641, [1,0,-1] 0.25, True
	Initial Structure	

Relaxed Structure

Figure S7: Three types of outliers detected during the analysis. Surface ID consists of MPID, miller index, shift value and orientation (True and False correspond to top and bottom of surface structures, respectively).
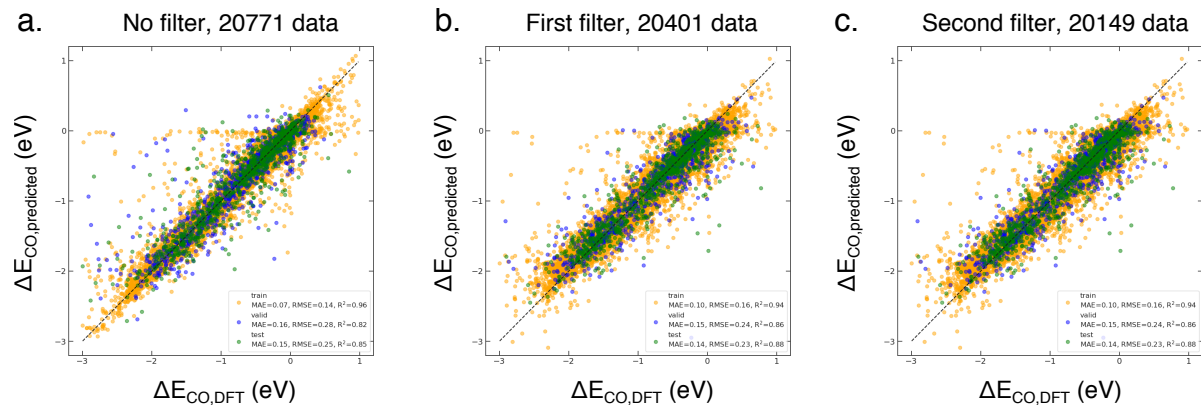
Figure S8: Two iterations of the outlier detection for CO binding energy prediction.
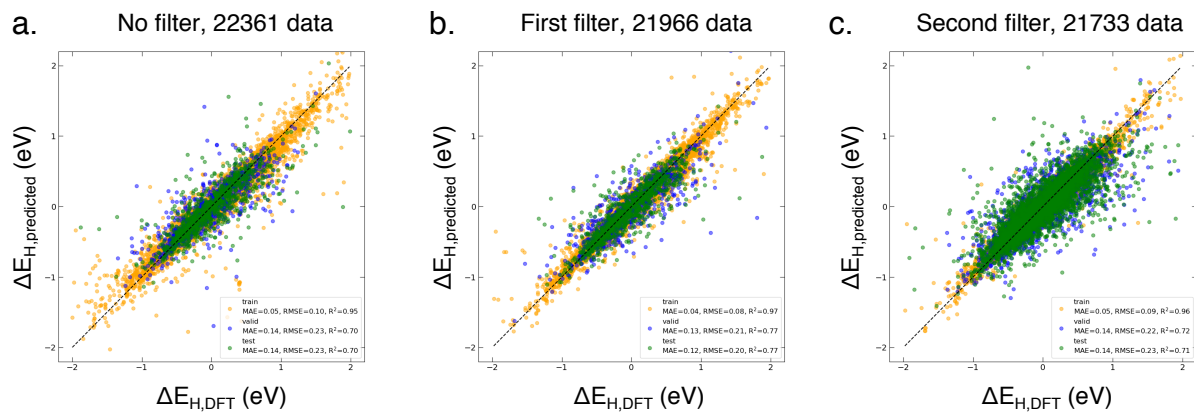

Figure S9: Two iterations of the outlier detection for H binding energy prediction.